Available online at www.sciencedirect.com
SCIENCE DIRECT®
C. R. Chimie 9 (2006) 676–683
COMPTES RENDUS CHIMIE
http://france.elsevier.com/direct/CRAS2C/

Full paper / Mémoire

Photoelectrochemical solar cells based on SnO_2 nanocrystalline films

Nguyen Nang Dinh [a], Marie-Claude Bernard [b], Anne Hugot-Le Goff [b,*], Thomas Stergiopoulos [c], Polycarpos Falaras [c]

[a] *Faculty of technology, Vietnam National University, 144, Xuan Thuy road, Cau-Giay District, Hanoi, Vietnam*
[b] *Laboratoire des interfaces et systèmes électrochimiques, UPR 15 du CNRS, université Pierre-et-Marie-Curie, 4, place Jussieu, 75252 Paris cedex 05, France*
[c] *Institute of Physical Chemistry, NCSR Demokritos, 15310 Aghia Paraskevi, Attikis, Athens, Greece*

Received 24 June 2004; accepted after revision 27 January 2005

Available online 09 September 2005

Abstract

Dye-sensitized solar cells (DSSCs) fabricated using nanocrystalline SnO_2 films sensitized by the Ru(dcbpy)$(NCS)_2$ dye (N3) were compared to the corresponding nanocrystalline titania cells. Although the light-to-power energy conversion efficiency of SnO_2 cells is low with respect to the nc-TiO_2 DDSCs, their general characteristics are similar. The influence of the addition of 4-*tert*-butylpyridine (4TBP) or acetic acid to the electrolyte was investigated. 4TBP increased the cell's open-circuit voltage and stability. Raman spectroscopy confirmed the presence of new vibration bands; their intensity depends on the additives and characterizes the amount of tri-iodides at the photoactive interface, as well the complex formed between dye and iodide. ***To cite this article: N. Nang Dinh et al., C. R. Chimie 9 (2006)***.

Résumé

Des cellules solaires utilisant l'oxyde d'étain nanocristallin, sensibilisées par le complexe de ruthénium N3: Ru(dcbpy)$(NCS)_2$ ont été comparées à leurs homologues utilisant l'oxyde de titane. Deux adjuvants, 4-*tert*-butylpyridine (4TBP) ou acide acétique, ont été ajoutés à l'électrolyte pour augmenter le potentiel en circuit ouvert de la cellule et sa stabilité à long terme. L'addition de 4TBP améliore nettement ces deux caractéristiques. On a utilisé la spectroscopie Raman pour caractériser les espèces à l'interface photoélectrode–électrolyte. L'apparition de nouvelles bandes de vibration (dont l'intensité dépend de l'adjuvant) permet de caractériser le complexe formé entre le colorant et l'oxyde, et d'estimer la quantité de tri-iodures présente à l'interface photoactive. ***Pour citer cet article : N. Nang Dinh et al., C. R. Chimie 9 (2006)***.

Keywords: Dye-sensitized solar cells; DSSC; SnO_2; N3; Raman spectroscopy; Photoelectrochemical efficiency

Mots-clés : Cellules solaires sensibilisées par colorant ; SnO_2 ; N3 ; Spectroscopie Raman ; Rendement photoélectrochimique

* Corresponding author.
E-mail addresses: nndinh@ims.ncst.ac.vn (N. Nang Dinh), ramanrt@ccr.jussieu.fr (A. Hugot-Le Goff), papi@chem.demokritos.gr (T. Stergiopoulos), papi@chem.demokritos.gr (P. Falaras).

1631-0748/$ - see front matter © 2005 Académie des sciences. Published by Elsevier SAS. All rights reserved.
doi:10.1016/j.crci.2005.02.042

1. Introduction

Taking into account the value of its bandgap, SnO_2 seems to be a good candidate for the dye-sensitized solar cells (DSSC); it can also be prepared in a convenient nanocrystalline form (nc-SnO_2) [1,2]. However, we will confirm here that the photoelectrochemical efficiency of nc-SnO_2 DSSCs is noticeably lower than the efficiency of nc-TiO_2 cells [3–11]. In the case of the nc-TiO_2 cells using N3 dye [N3: (*cis*-bis(isothiocyanato)bis(2,2′-bipyridine-4,4′-dicarboxylic acid)-Ru(II)], one knows that one of the reasons for their high efficiency is the excellent grafting between the terminal group of the bridging ligand, COOH, and the surface of anatase, which optimizes the electron injection.

We tried to add different additives in the electrolyte, able to improve the cell efficiency by modifying in particular the tri-iodides amount at the interface. The most studied additive is 4-*tert*-butylpyridine (4TBP), it was shown that the exposure of the dye-photoelectrode to 4TBP improves the fill factor (FF) and open-circuit voltage (V_{oc}) of the device without affecting the short-circuit photocurrent (J_{sc}). The increase of V_{oc} is due to the suppression of the dark current (arising from the reduction of triiodide by conduction band electrons, which occurs despite the fact that the TiO_2 surface is covered by a dye monolayer) at the semiconductor electrolyte interface. 4TBP is adsorbed at the TiO_2 surface and this blocks surface states, thus resulting to a decrease in the rate of reduction of triiodide by conduction band electrons [12,13]. Here, we will study also the influence of the acetic acid (AcH) which blocks the semiconductor surface and hinders the charge transfer process between the injected electron and the triiodides [14].

2. Experimental

2.1. SnO_2

To obtain high conversion efficiency, the preparation of rough, high surface area nano-structured thin films is necessary. Transparent nc-SnO_2 thin film electrodes were prepared by doctor-blading a colloid solution of 15 wt % tin oxide (Nyacol Products) in water on SnO_2:F conductive glass substrates, followed by a thermal treatment of sintering at 450 °C in air for 30 min. The investigation of their morphological properties by SEM showed that uniform and well-crystallized nc-SnO_2 films were obtained, with good adherence and a critical thickness, which is not larger than 2.0 μm. We have compared the photoelectrochemical properties of 1.5μm- and 2.46μm-thick films, the thicker film are better, but the differences are not so great. The results given here were obtained with a 1.5μm-thick film. Fractal analysis leads to a fractal dimension of 2.368, proving a self-similar and self-affine character of significant complexity.

2.2. Surface modification

Here we have used exclusively N3 dye from Solaronix. Surface derivatization of tin oxide was achieved by immersing the SnO_2 thin-film electrodes (heated at 120 °C) overnight in a 10^{-4} M ethanolic solution of this complex. It is noteworthy that a red coloration color developed immediately after immersion, confirming the dye grafting on the semiconductor surface. After completion of the dye adsorption the modified materials were thoroughly washed with ethanol and dried. Thus, any dye in excess (physically adsorbed) was eliminated and a monolayer coverage was ensured.

2.3. Electrolyte and cell elaboration

Counter electrode is a similar SnO_2:F coated substrate that had been platinized by DC-sputtering deposition, to give a catalytic effect on the electron donor reduction. The electrolyte is sandwiched between the dye-sensitized tin oxide photoelectrode and the counter electrode. A spacer (thickness about 50 μm) is placed between the two electrodes to avoid short-circuiting and to ensure the thickness of the electrolyte. The liquid electrolyte consists of propylene carbonate (PC), in which the redox couple LiI + I_2 is added. Here, we used a total amount of iodine of 0.12: 0.1 M LiI + 0.01 M I_2. Respectively 0.17 M acetic acid (AcH) or 0.1 M 4TBP were added.

We must point that the electrolyte composition was chosen in order to allow the best Raman and optical analysis, which requires to have a not too optically absorbing electrolyte, and therefore to limit the iodine concentration. In the present experiments, the electrolyte is therefore far from to be optimized in iodine, and the efficiencies will be subsequently very low.

2.4. Raman spectroscopy

The photoelectrochemical performances of the DSSC using visible light were first investigated. Then the Raman spectra of cells were collected using a Jobin-Yvon LABRAM confocal device with a green exciting light (514.5 nm) of low intensity, in a large potential range (–0.5 V to + 0.5 V). We have shown in the case of nc-TiO_2 cells that this technique allowed to study in the same time the formation of triiodides and of a complex between pyridine and iodide [15,16], possible modification of the dye through shifting of its bands [17] and modifications of the oxidation state of the thiocyanate ligand [15].

3. Results

3.1. Photoelectrochemical performances

Figs. 1–3 show the current-voltages characteristics of DSSC in absence of additive (Fig. 1), in presence of AcH (Fig. 2) and in presence of 4TBP (Fig. 3). The dark current is given in dashed line. The different calculated parameters are given in legend: voltage in open circuit V_{oc}, current of short circuit J_{sc}, fill factor FF, energy conversion efficiency GPE. The energy conversion efficiency is 0.05% in presence of AcH and 0.3% in presence of 4TBP, which demonstrates the large improvement of the cell photoelectrochemical performances due to this adjuvant.

Characterization of optical and photoelectrochemical properties of the nc-SnO_2 DSSCs in comparison

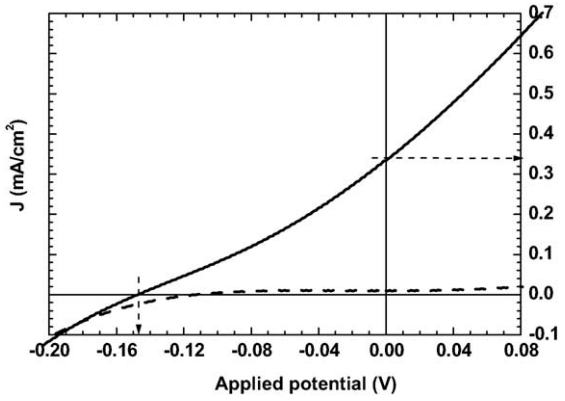

Fig. 1. Current–voltage characteristics of N3/SnO_2 DSSC: V_{oc} = 0.146 V; J_{sc} = 0.34 mA/cm^2 FF = 0.16, GPE = 0.02%.

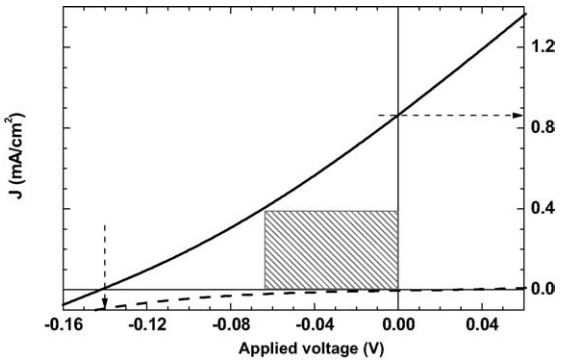

Fig. 2. Current–voltage characteristics of N3/SnO_2 DSSC with added AcH. P_{in} = 56 mW/cm^2, V_{oc} = 0.14 V, J_{sc} = 0.86 mA/cm^2, FF = 0.22, GPE = 0.05%.

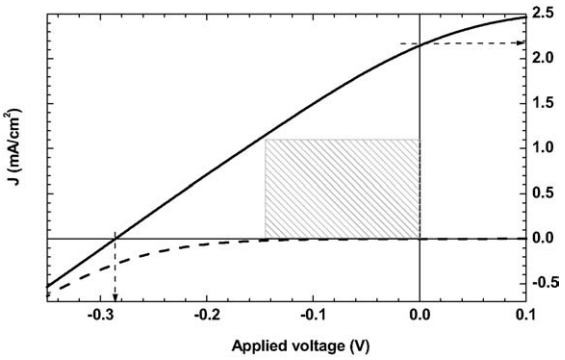

Fig. 3. Current–voltage characteristics of N3/SnO_2 DSSC with added 4TBP. P_{in} = 56 mW/cm^2, V_{oc} = 0.285 V, J_{sc} = 2.2 mA/cm^2, FF = 0.27, GPE = 0.3%.

with nc-TiO_2 DSSCs, whose characteristics in presence of 4TBP are given in Fig. 4, has shown that nc-SnO_2 electrodes exhibit poorer photoconversion efficiencies than those obtained with nc-TiO_2 photoan-

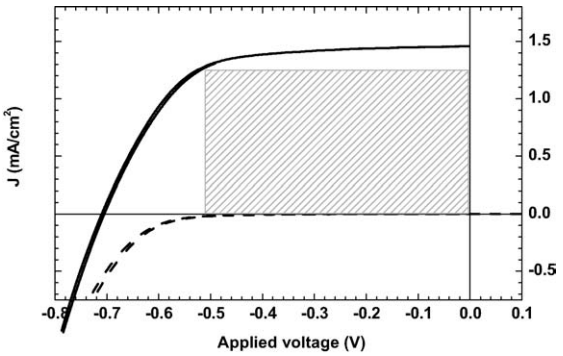

Fig. 4. Current–voltage characteristics of N3/TiO_2 DSSC with added 4TBP. P_{in} = 56 mW/cm^2, V_{oc} = 0.71 V, J_{sc} = 1.5 mA/cm^2, FF = 0.62, GPE = 1.2%.

odes (in the case of nc-TiO_2, the energy conversion efficiency is 1.2%). From the slope of the quasi-linear current voltage curves in Figs. 1–3, the internal series resistance was obtained as high as 500, 165, 135 Ω cm^2 for N3/SnO_2 without additive, N3/SnO_2 with AcH, N3/SnO_2 with 4TBP respectively. From the corresponding slope of the linear part of the current voltage curve in Fig. 4, the value of internal series resistance was determined to be less than 100 Ω cm^2 for N3/TiO_2 (with 4TBP). A higher ohmic drop shifts the photocurrent plateau towards positive potentials and is the main cause for poor cell's efficiency. The low light-to-power energy conversion efficiency connected to the low fill factors and photovoltages can be due to the intrinsic properties of tin oxide, to a bad bridging between N3 and SnO_2 or to a bad effect in the reduction of triodides by conduction band electrons. We used Raman spectroscopy to try to elucidate this point.

3.2. Raman results

Recent investigations on dye-sensitized TiO_2 solar cells by resonance Raman spectroscopy revealed the presence of new vibration bands in the low wavenumber region. These bands were observed using a number of different dye/TiO_2/electrolyte combinations and were attributed to new species formed during the cell's operation. We have shown in [15,16] that the presence of triiodides at the photoactive electrode was detected by a strong band at 112 cm^{-1}, while another band at 167 cm^{-1} could be assigned to symmetric ν(I–I) in a complex formed between the oxidized form of the dye and iodides and a smaller band at 138 cm^{-1} to the corresponding asymmetric stretching [18]. In the previous case, these bands could be really quantitatively used, in reason of the strong anatase band at 143 cm^{-1}. In the present work, we confirmed the general character of the phenomenon by replacing the titania film by tin oxide, a semiconductor that can be considered as a better electron acceptor than TiO_2. Here, the results will be presented after a normalization by the strongest dye band at 1544 cm^{-1}, which is not fully satisfying. Apart the identification and potential dependence of the two iodides bands, we look also at the dye spectrum and specially at the faint NCS stretching band. This ligand of low electronegativity is in fact believed to participate with Ru to the HOMO and therefore to play an important role in the complex stabilization, facilitating the dye regeneration by the redox couple. It is assumed in the literature [19,20] to have a predominant role in the abundance of iodides at the interface.

3.2.1. Influence of the iodide content in electrolyte (N3/TiO_2 DSSC)

To illustrate the importance of the role played by the amount of iodide added to the electrolyte, we have plotted in Fig. 5 the normalized intensities of these two bands in N3/nc-anatase cells; the redox couples added to the PC electrolyte were respectively: circles, 0.01 M LiI + 0.001 M I_2; diamonds, 0.1 M LiI + 0.01 M I_2; squares, 0.5 M LiI + 0.05 M I_2; the dashed vertical line separates the photocurrent plateau range from the recombination range in the left. While tri-iodides are present at every potential if the amount of iodide added

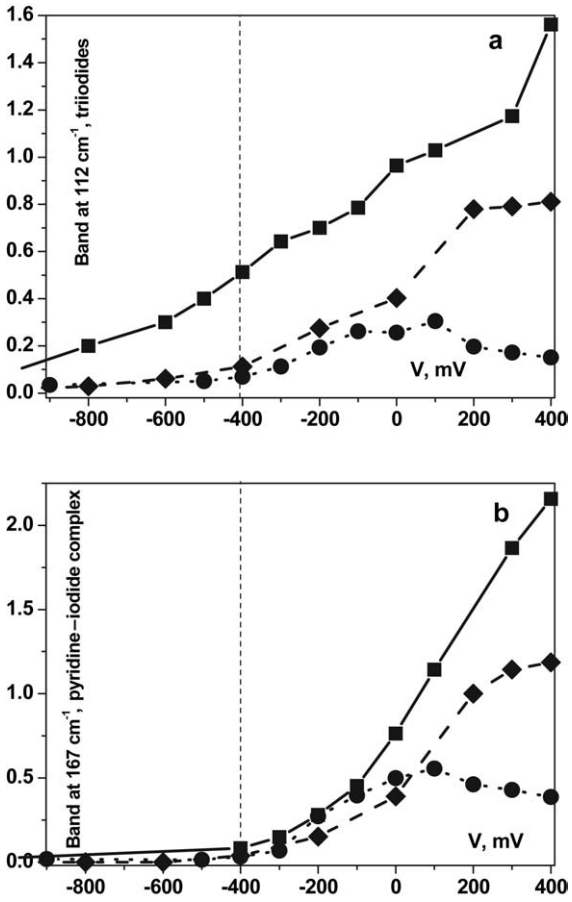

Fig. 5. Intensities of the low wavenumbers bands (after normalization by the main dye band) in N3/TiO_2 DSSC with different iodide contents in the electrolyte: dots/circles, 0.012 M; dashes/diamonds, 0.12 M; solid line/squares, 0.6 M.

to electrolyte is too large, the complex is formed only in presence of photocurrent, therefore of oxidized form of the dye, which checks its formation by the intermediate of the D^+ species. With lowest concentration in iodide, the decrease of bands at high potential shows that this concentration is not enough to ensure the regeneration of DSSC. This study served us to choose the right redox couple concentration in the N3/nc-anatase cells, which we have kept in the present study.

In Fig. 6, we have plotted the intensity (6a) and frequency (6b) of the bands assigned to the SCN stretching for iodide concentrations of 0.012 M (circles) and 0.6 M (squares). It is obvious that the band is not modified by the more or less great amount of iodide at the interface; a striking point is the shift of this vibration which passes from 2104 cm^{-1} that is its normal value [19] to 2129/2130 cm^{-1} in the photocurrent region where dye is oxidized.

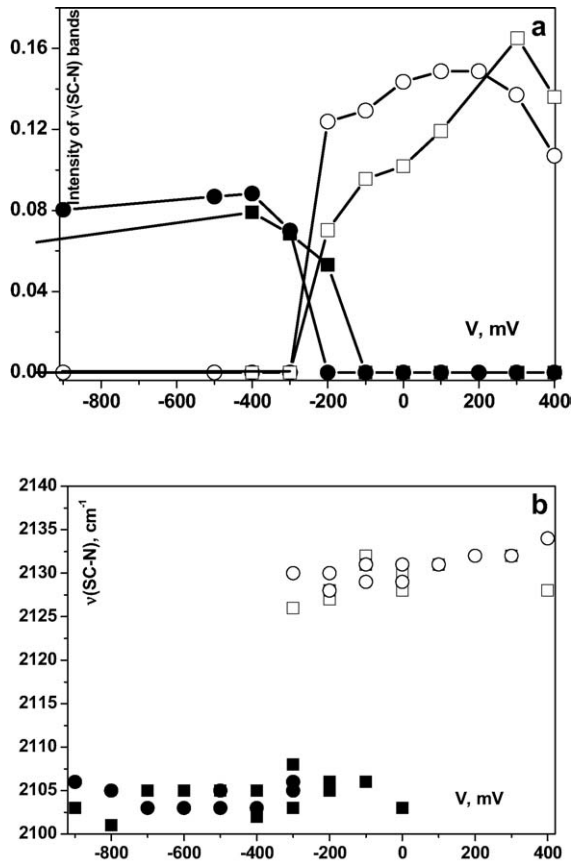

Fig. 6. Intensities (after normalization by the main dye band) (**a**) and wavenumbers (**b**) of the bands (full symbols: 2104 cm^{-1}; open symbols: 2130 cm^{-1}) due to the stretching of the SCN group in N3/TiO_2 DSSC; circles: 0.012 M; squares: 0.6 M.

3.2.2. *Influence of the additives in electrolyte (N3/SnO_2 DSSC)*

The Fig. 7 allows to summarize the effect of the two additives on the iodide species at the interface.

The effect of AcH is obvious, but limited to the high potential range. As shown in Figs. 1–2, its main effect was to increase J_{sc}. It slightly decreases the amount of triiodide (7a), but over all it plays a noticeable role on the formation of complex between the dye and I_2 (7b). That seems coherent with some blocking effect of the charge transfer process.

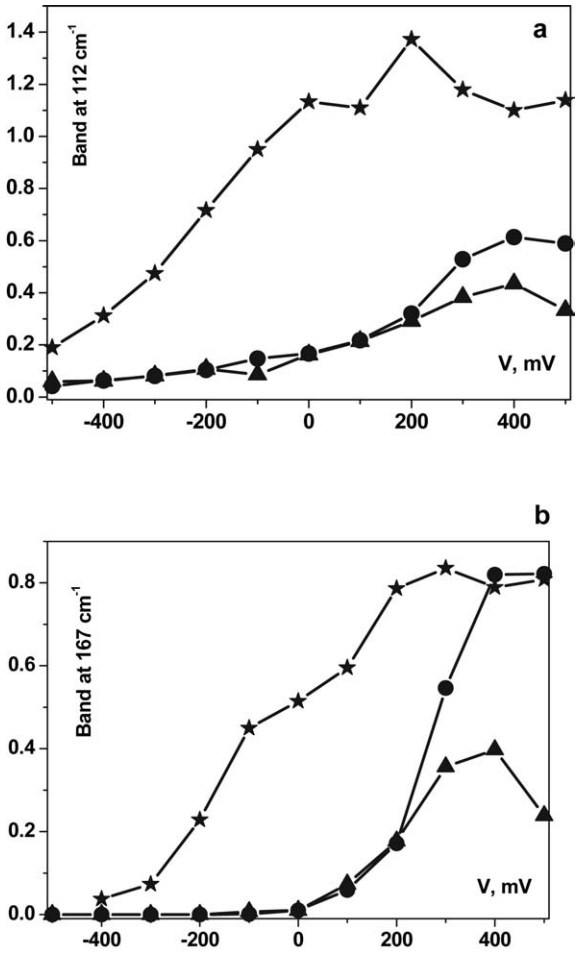

Fig. 7. Intensities (after normalization by the main dye band) of the low wavenumber bands: (**a**), tri-iodides, (**b**) species formed between pyridine and iodide in N3/SnO_2 DSSC with 0.12 M iodide; circles: without additive; triangles: in presence of AcH; stars: in presence of 4TBP.

On the contrary, 4TBP gives a noticeable effect. One saw that it allowed a gain of about 160 mV in the open-circuit potential, but one sees in Fig. 7b that the formation of DI^+ complex is shifted of more than 400 mV. Over all, one sees that triiodides are present at the interface in the whole potential range in a very high amount, comparable to the amount observed in presence of 0.6 M iodides in the electrolyte. Since the efficiency of cells with 0.6 M iodides is better than the efficiency of cells with the present iodide concentration (0.12 M), the connection is established between the benefic effect on the efficiency of 4TBP and the enhancement of the tri-iodides interfacial species: the rate of reduction of triiodide is actually reduced.

The SCN band is generally low in the dye spectrum when it is deposited on SnO_2. However, on can see in Fig. 8 which compares this band in cells with and without 4TBP (the intensities of features at 2007 and 2134 cm^{-1} are not separated in the figure because of the broadness of bands), that the general behavior remains the same, but that the vibration is quite quenched in presence of 4TBP. This adjuvant has therefore a deep influence on the interface, as checked by Fig. 9, in which the Raman spectrum in presence of 4TBP (solid line) is compared with the spectrum of DSSC without adjuvant, in the wavenumber range of the main vibrations of the pyridine ring. The band at 1544 cm^{-1} can be split into two parts with a new component appearing at 1525 cm^{-1}, and another small band appears at 1580 cm^{-1}. These bands (ν_5 and ν_6) are the corresponding of the normal ν_5 and ν_6 vibrations (stretching of C=C). Their appearance indicates that in presence of 4TBP, there are two different carbon sites, one ensuring the normal grafting via the COOH group, and the other giving evidence in the formation of interaction between pyridine and 4TBP.

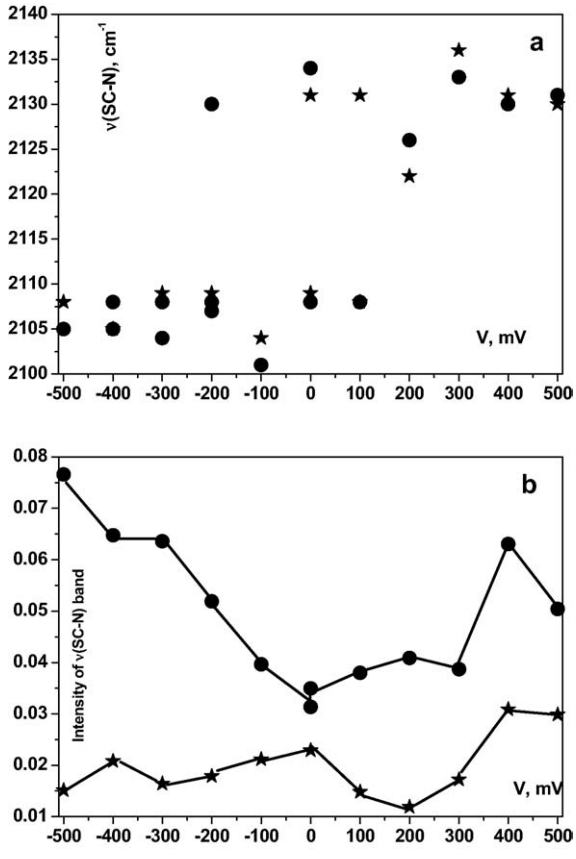

Fig. 8. Wavenumbers (**a**) and intensities after normalization by the main dye band (**b**) of the bands due to the stretching of the SCN group in N3/SnO_2 DSSC with 0.12 M iodide; circles: without additive; stars: in presence of 4TBP.

On the contrary, the spectra obtained in presence of AcH are strictly identical to the spectra of cell without additive.

These observations are, at the present time, not easy to analyze, but they do not go in the sense proposed by Greijer et al. [19,20] which are, at our knowledge, alone in the literature to try to explain the 4TBP influence. They think that 4TBP decreases the triiodide concentration in the oxide film, and improves the open circuit voltage of the cell, since the reaction between injected electrons and I_3^- is reduced. They propose a mechanism of thiocyanate ligand exchange and consider that

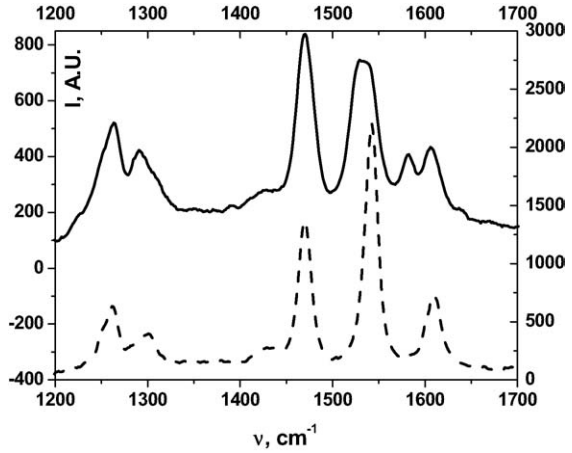

Fig. 9. Raman spectra of N3/SnO_2 DSSC with 0.12 M iodide polarized at 0 mV, without (dashed line) and with (solid line) 4TBP.

4TBP suppresses the loss of the SCN ligand, improving therefore dye stability. The present results go in the sense of an enhancement of iodides concentration, and an interaction with pyridine ring rather than with SCN.

4. Discussion

Direct comparison between TiO_2 and SnO_2 (with 0.12 M iodine) proves that the nature of the semiconductor does not influence the Raman behavior. In fact, the ratio of the corresponding peaks is the same for triiodides, dye-triiodide complex and SCN stretching.

Increase of iodine (I_2) causes increase of triiodides in both anodic and cathodic domain (TiO_2). A similar increase is observed by addition of 4TBP (SnO_2). This can be explained if one takes into account that equilibrium exists between iodides and triiodides:

$$I^- + I_2 \rightleftharpoons I_3^- \quad (1)$$

However, it is well known that 4TBP reacts with iodine [19] following the reactions:

$$(4TBP) + I_3^- \rightleftharpoons (4TBP)I_2 + I^- \quad (2)$$

$$2\,(4TBP) + I_3^- \rightleftharpoons (4TBP)_2I^+ + 2\,I^- \quad (3)$$

Reactions (2) and (3) will increase the concentration of iodides (I^-). This may cause a shift of equilibrium of equation (1) on the right side, so increase of concentration of triiodides (I_3^-). As a result the Raman vibration band of triiodide species significantly increases by addition of 4TBP. Increase of the concentration of the triiodides may result in a parallel increase of the intensity of the 167 cm^{-1} vibration band (attributed to the formation of an intermediate complex: $[D^+]I_3^-$ between the dye and the triodides [16]. The phenomenon is more intense in the anodic range, where the stabilization of $[D^+]I_3^-$ species is easier. Such a species can be involved in and facilitate the dye regeneration, thus affecting not only the photocurrent but also the photovoltage and therefore considerably improving the cell parameters.

The addition of AcH does not seem to have similar effects. This can be understood, if one considers that AcH cannot take part in similar reactions (reactions 2 and 3). The positive role of the AcH addition is limited to reduce the charge recombination process, via its adsorption on the semiconductor surface.

5. Conclusion

AcH added to N3/SnO_2 DSSC has a limited effect, increasing the short-circuit current and decreasing slightly the iodides at the interface. 4TBP has an effect on the open circuit potential, allows a significant increase of the GPE but Raman spectroscopy shows that it modifies deeply the photoactive interface. Unfortunately, even with 4TBP the filling factor is so small that the cell performances are far from reaching the N3/TiO_2 DSSC efficiency values.

In Fig. 10 are summarized some Raman and photoelectrochemical results, compared with N3/TiO_2 DSSC characteristics. In the case of these cells, their greater efficiency is related essentially to higher values of open-circuit potential: 0.6 V (more than 0.7 V with 4TBP) instead of, at the maximum, 0.285 V with 4TBP when SnO_2 is used, and to higher values of fill factor. The

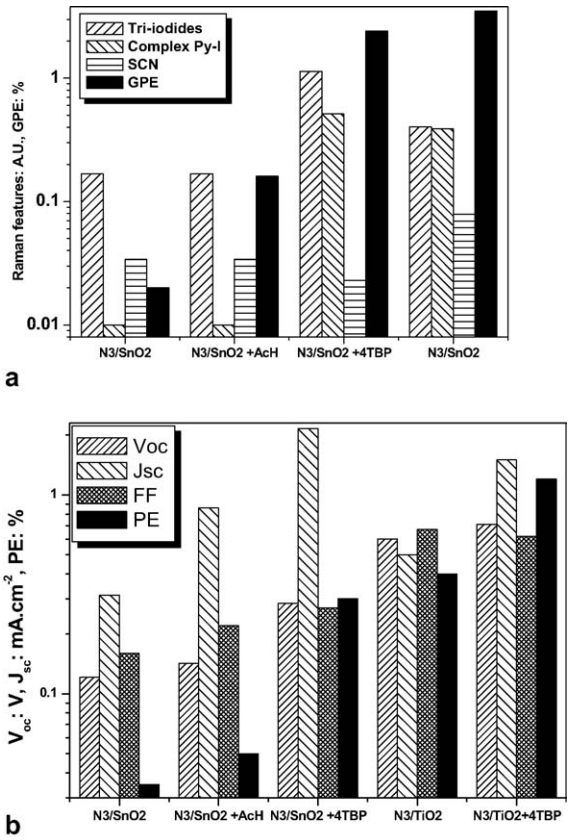

Fig. 10. Schematic representation of Raman and photoelectrochemical results obtained with nc-SnO_2 DSSCs, compared with the corresponding data for nc-TiO_2 DSSCs. (**a**) Raman results and GPE; (**b**) other photoelectrochemical characteristics.

additives have over all a beneficial action on the efficiency through the enhancement of J_{sc}, which is not the prime parameter. The Raman features originating in iodides increase in the same time that J_{sc}. In the same time, there is a small decrease of isothiocyanate response. 4TBP is clearly associated to an increase of the tri-iodides band and therefore to an hindering of its reduction.

References

[1] K. Tennakone, P.K.M. Bandaranayake, P.V.V. Jayaweera, A. Konno, G.R.R.A. Kumara, Physica E 14 (2002) 190 (Amsterdam).

[2] P.V. Kamat, I. Bedja, S. Hotchandani, L.K. Patterson, J. Phys. Chem. 100 (1996) 4900.

[3] J. Bandara, K. Tennakone, P.P.B. Jayatilaka, Chemosphere 49 (2002) 439.

[4] F. Fungo, L.A. Otero, L. Sereno, J.J. Silber, E.N. Durantidi, J. Mater. Chem. 10 (2000) 645.

[5] C. Nasr, P. Kamat, S. Hotchandani, J. Phys. Chem. B 102 (1998) 10047.

[6] K. Hara, T. Horiguchi, T. Kinoshita, K. Sayama, H. Sugihara, H. Arakawa, Sol. Energ. Mat. Sol. C. 64 (2000) 115.

[7] D.N. Srivastava, S. Chappel, O. Palchik, A. Zaban, A. Gedanken, Langmuir 18 (2002) 4160.

[8] S. Ferrere, A. Zaban, B.A. Gregg, J. Phys. Chem. B 101 (1997) 4490.

[9] H. Tian, P.-H. Liu, F.-S. Meng, E. Gao, S. Cai, Synthetic Met. 121 (2001) 1557.

[10] S. Chappel, A. Zaban, Sol. Energ. Mat. Sol. C. 71 (2002) 141.

[11] A. Kay, M. Grätzel, Chem. Mater. 14 (2002) 2930.

[12] M.K. Nazeeruddin, P. Pechy, T. Renouard, S.M. Zakeeruddin, R. Humphry-Baker, P. Comte, P. Liska, L. Cevey, E. Costa, V. Shklover, L. Spiccia, G.B. Deacon, C.A. Bignozzi, M. Grätzel, J. Am. Chem. Soc. 123 (2001) 1613.

[13] S.Y. Huang, G. Schlichthörl, A.J. Nozik, M. Grätzel, A.J. Frank, J. Phys. Chem. B 101 (1997) 2576.

[14] T.S. Kang, K.H. Chun, J. Hong, S.H. Moon, K.J. Kim, J. Electrochem. Soc. 147 (2000) 3049.

[15] M.C. Bernard, H. Cachet, P. Falaras, A. Hugot-Le Goff, M. Kalbac, I. Lukes, N.T. Oanh, T. Stergiopoulos, I. Arabatzis, J. Electrochem. Soc. 150 (2003) E155.

[16] T. Stergiopoulos, M.C. Bernard, A. Hugot-Le Goff, P. Falaras, Coord. Chem. Rev. (2004) (in press).

[17] T. Stergiopoulos, M.C. Bernard, A. Hugot-Le Goff, P. Falaras, Abstracts 203th Electrochem. Soc. Meeting, Paris, 2003.

[18] A. Hugot-Le Goff, S. Joiret, P. Falaras, J. Phys. Chem. B 103 (1999) 9569.

[19] H. Greijer, J. Lindgren, A. Hagfeldt, J. Phys. Chem. B 105 (2001) 6314.

[20] H. Greijer Agrell, J. Lindgren, A. Hagfeldt, Sol. Energy 75 (2003) 169.